The EMBO Journal (2009) 28, 3564–3578 | © 2009 European Molecular Biology Organization | All Rights Reserved 0261-4189/09
www.embojournal.org

THE EMBO JOURNAL

Synapse formation regulated by protein tyrosine phosphatase receptor T through interaction with cell adhesion molecules and Fyn

So-Hee Lim[1,3], Seok-Kyu Kwon[2], Myung Kyu Lee[1], Jeonghee Moon[1], Dae Gwin Jeong[1], Eunha Park[1], Seung Jun Kim[1], Byung Chul Park[1], Sang Chul Lee[1], Seong-Eon Ryu[1], Dae-Yeul Yu[1], Bong Hyun Chung[1], Eunjoon Kim[2], Pyung-Keun Myung[3] and Jae-Ran Lee[1,*]

[1]Brain Research Center, Korea Research Institute of Bioscience and Biotechnology, Daejeon, Republic of Korea, [2]Department of Biological Sciences, Korea Advanced Institute of Science and Technology, Daejeon, Republic of Korea and [3]College of Pharmacy, Chungnam National University, Daejeon, Republic of Korea

The receptor-type protein tyrosine phosphatases (RPTPs) have been linked to signal transduction, cell adhesion, and neurite extension. PTPRT/RPTPρ is exclusively expressed in the central nervous system and regulates synapse formation by interacting with cell adhesion molecules and Fyn protein tyrosine kinase. Overexpression of PTPRT in cultured neurons increased the number of excitatory and inhibitory synapses by recruiting neuroligins that interact with PTPRT through their ecto-domains. In contrast, knockdown of PTPRT inhibited synapse formation and withered dendrites. Incubation of cultured neurons with recombinant proteins containing the extracellular region of PTPRT reduced the number of synapses by inhibiting the interaction between ecto-domains. Synapse formation by PTPRT was inhibited by phosphorylation of tyrosine 912 within the membrane–proximal catalytic domain of PTPRT by Fyn. This tyrosine phosphorylation reduced phosphatase activity of PTPRT and reinforced homophilic interactions of PTPRT, thereby preventing the heterophilic interaction between PTPRT and neuroligins. These results suggest that brain-specific PTPRT regulates synapse formation through interaction with cell adhesion molecules, and this function and the phosphatase activity are attenuated through tyrosine phosphorylation by the synaptic tyrosine kinase Fyn.

The EMBO Journal (2009) **28,** 3564–3578. doi:10.1038/emboj.2009.289; Published online 8 October 2009
Subject Categories: signal transduction; neuroscience
Keywords: cell adhesion molecule; Fyn; PTPRT; synapse formation; tyrosine phosphorylation

*Corresponding author. Brain Research Center, Korea Research Institute of Bioscience and Biotechnology, Daejeon 305-806, Republic of Korea. Tel.: +82 42 879 8437; Fax: +82 42 860 4598;
E-mail: leejr@kribb.re.kr

Received: 4 August 2009; accepted: 7 September 2009; published online: 8 October 2009

Introduction

The functions of PTPRT/RPTPρ, a protein tyrosine phosphatase (PTP) expressed only in the brain, have not been defined, although several potential substrates have been suggested (Besco *et al*, 2006; Zhang *et al*, 2007). PTPRT is a classical PTP that has a core cysteine residue in the active site and is localized in the plasma membrane by its trans-membrane domain (McAndrew *et al*, 1998; Paul and Lombroso, 2003; Besco *et al*, 2004; Sallee *et al*, 2006). PTPRT is classified in the same subfamily as PTPRK, PTPRM, and PTPRU (PCP-2), all of which have a common MAM domain in the extracellular N-terminus followed by one Ig and several FN domains. PTPRT has two intracellular catalytic domains; the membrane–proximal catalytic domain is active, whereas its membrane distal catalytic domain is inactive similar to many other PTPs (Alonso *et al*, 2004). Several PTPRT gene mutations have been found in colon cancer, and transformation could be inhibited by overexpression of wild-type (WT) PTPRT (Wang *et al*, 2004). However, based on *in situ* hybridization data, PTPRT has a brain-specific expression pattern in contrast with PTPRK, PTPRM, and PTPRU (Paul and Lombroso, 2003; Besco *et al*, 2004).

Several PTPs are reported to control axonal outgrowth, guidance, and synapse formation in the central nervous system (CNS), but many PTP-knockout mice have not shown significant phenotypes because PTP has many subfamilies in the brain that can compensate for the knockdown activity (Burden-Gulley and Brady-Kalnay, 1999; Harroch *et al*, 2000; Xie *et al*, 2001; Johnson and Van Vactor, 2003; Petrone *et al*, 2003; Dunah *et al*, 2005; Uetani *et al*, 2006). It has been questioned whether PTP has substrate specificity because structural analyses have not shown large differences among the catalytic domains of PTPs (Hoffmann *et al*, 1997; Nam *et al*, 1999, 2005; Johnson and Van Vactor, 2003; van Montfort *et al*, 2003). PTP is thought to have limited access to the phospho-tyrosine residues of substrates, and fine regulation of its activity may be accomplished by interaction with partners. PTP activity can be regulated by alternative splicing, modulation of protein levels, posttranslational modifications, dimerization, and subcellular localization (Paul and Lombroso, 2003; van Montfort *et al*, 2003). Especially, dimerization and active-site blockage was proposed for downregulating the catalytic activity of receptor-type PTP (RPTPα) and other RPTPs (Bilwes *et al*, 1996). The wedge formed by amino-terminal helix-turn-helix segment of RPTPα D1 inserts into the active site of a dyad-related D1 monomer, which would block the access of the substrates. Some PTPs communicate with protein tyrosine kinase (PTK) directly or indirectly, but it is rare for PTP activity to be controlled by PTK; PTK is activated by PTP in many cases (Zeng *et al*, 1999; Tsujikawa *et al*, 2002; Berman-Golan and Elson, 2007). Despite the likelihood that tyrosine phosphorylation

occurs in PTP, auto-dephosphorylation would make it difficult to detect.

Homophilic or heterophilic interactions among the ecto-domains of cell adhesion molecules are well characterized for both *cis*- and *trans*-interactions (Boggon *et al*, 2002; Dean *et al*, 2003; Boucard *et al*, 2005; Kim *et al*, 2006). Trans-synpatic interaction between neuroligin and neurexin is known to regulate synapse formation and synaptic functions at excitatory and inhibitory synapses (Graf *et al*, 2004; Chih *et al*, 2005; Chubykin *et al*, 2007; Sudhof, 2008). However, signal transduction mechanisms that regulate the functions of neuroligins and neurexins have not been identified (Dean and Dresbach, 2006; Craig and Kang, 2007). Some RPTPs have ecto-domains similar to those of cell adhesion molecules, and likely interact with other RPTPs or cell adhesion molecules through these ecto-domains. The extracellular ecto-domains of RPTP are highly divergent and consist of a wide variety of different structural motifs, whereas the cytoplasmic catalytic domains are conserved. However, heterophilic interactions through the ecto-domain of RPTP have not been reported except in PTPσ, PTPζ/β, and LAR (Brady-Kalnay *et al*, 1995; Gebbink *et al*, 1995; Krasnoperov *et al*, 2002; Johnson and Van Vactor, 2003; Anders *et al*, 2006; Woo *et al*, 2009). The ecto-domains of PTPRK and PTPRM failed to interact in a heterophilic manner despite their structural similarity (Zondag *et al*, 1995). PTPRM is known to interact with E-cadherin through intracellular domains, not ecto-domains (Brady-Kalnay *et al*, 1995). When RPTPs interact with cell adhesion molecules through ecto-domains, many cytoplasmic substrates could be made accessible to RPTPs for further signal transduction.

In this study, the functions of PTPRT in the brain were investigated. When overexpressed, PTPRT increased the density of dendritic spines and excitatory and inhibitory synapses in cultured neurons. Knockdown of PTPRT resulted in a decrease in the number of dendritic spines and excitatory synaptic transmission. The soluble PTPRT ecto-Fc protein reduced the number of dendritic spines and excitatory synapses by inhibiting the interaction between ecto-domains. Endogenous interaction partners of PTPRT were examined in the rat brain synaptosome by immunoprecipitation using a PTPRT-specific monoclonal antibody and tandem mass spectrometry for amino acid sequencing. As a result, neuroligin was identified as a candidate interaction partner of PTPRT. Both neuroligin and neurexin interacted with PTPRT through the extracellular ecto-domains. Neuroligin was recruited by overexpressed PTPRT and synapse formation by neuroligin was not induced when PTPRT was knocked down in cultured neurons. A specific tyrosine residue (Y912) in the wedge formed by helix-turn-helix segment of PTPRT catalytic domain was found to be phosphorylated by Fyn. The clashes of phosphorylated tyrosine with the surrounding residues would help the wedge into the catalytic pocket of other monomer and strengthen the dimeric interaction. An *in vitro* PTP assay showed that the catalytic domain of a PTPRT phosphorylation-mimic mutant (Y912E) had a severely reduced activity. Fyn interfered with synapse formation by increasing homophilic interactions of PTPRT and by inhibiting interaction between PTPRT and neuroligin. PTPRT-induced synapse formation was attenuated by co-expression with Fyn and the augmentation of synapses did not occur when neurons were transfected with PTPRT mutant mimicking phosphorylation. Thus, brain-specific PTPRT/RPTPρ regulates synapse formation by gaining access to synaptic substrates connected with cell adhesion molecules, and its activity seems to be regulated through tyrosine phosphorylation by Fyn PTK.

Results

PTPRT is localized in the brain and neuronal synapses

According to *in situ* hybridization data, PTPRT is expressed only in the CNS in contrast to PTPRM, PTPRK, and PTPRU (PCP-2), which are ubiquitously expressed in many organs. A PTPRT-specific monoclonal antibody was produced against the catalytic domain, and was shown to recognize only recombinant PTPRT but not PTPRM, PTPRK, or other PTPs (Supplementary Figures S1A and B). When overexpressed in heterologous cells, only PTPRT reacted with the monoclonal antibody, but PTPRM, PTPRTK, or PTPRU did not (Figure 1A) (Jiang *et al*, 1993). In mouse samples, PTPRT proteins appeared as two major bands, similar to other members of this protein subfamily (Brady-Kalnay *et al*, 1995): a full-length 210 kDa form and a cleaved 110 kDa form. These forms were detected only in the brain, similar to the brain-specific scaffolding protein post-synaptic density-95 (PSD-95) (Figure 1B). To understand the nature of short form, a predicted cleavage site for furin in PTPRT was changed (Mut-PTPRT; K635N, R637L) (Figure 1C). The short form (indicated by an arrowhead) disappeared by the mutation of the furin-cleavage site (KSRR→NSLR). In the early development stages of the rat brain, another 90 kDa cleavage fragment or possible alternative splicing form of PTPRT was evident, but the expression level of full-length (210 kDa) and 110 kDa proteins gradually increased up to the 3 weeks of age, whereas the expression of the 90 kDa fragment became undetectable from 3 weeks (Figure 1D) (Besco *et al*, 2004). In subcellular fractions of the brain, the majority of PTPRT proteins were localized in the synaptosomal (P2), crude microsome (P3), synaptic plasma membrane (LP1), and synaptic vesicle (LP2) fractions (Figure 1E). In PSD fractions, PTPRT was retained in the PSD III, although it was not enriched to the same extent as PSD-95.

In brain slices, PTPRT monoclonal antibodies revealed PTPRT expression in specific brain regions (F2), whereas signals could not be detectable in the kidney (a negative control tissue) (F4) (Figure 1F). PTPRT signals were eliminated when PTPRT monoclonal antibodies were pre-incubated with cognate antigen proteins (G4) (Figure 1G). In cultured hippocampal neurons, PTPRT was present in both neurons and astrocytes, marked by staining for MAP2 and GFAP, respectively (Figure 1H and I). PTPRT was localized to dendritic spines, marked by PSD-95 (Figure 1J) and soluble RFP (Supplementary Figure S1D) (arrowhead). PTPRT co-stained with the representative synaptic markers synaptophysin and PSD-95 and appeared to be localized to neuronal synapses (Figure 1K and L, arrowhead). When EGFP-tagged PTPRT was expressed in cultured neurons, PTPRT was shown to co-localize with PSD-95 and vGLUT, which are markers for excitatory synapses (Figure 1M, arrowhead). PTPRT was also localized to inhibitory synapses stained with gephyrin and vGAT (Figure 1N, arrowhead).

PTPRT induces synapse formation in hippocampal-cultured neurons

We next tested whether overexpression of PTPRT has any effects on neuronal synapses (Figure 2). The density of

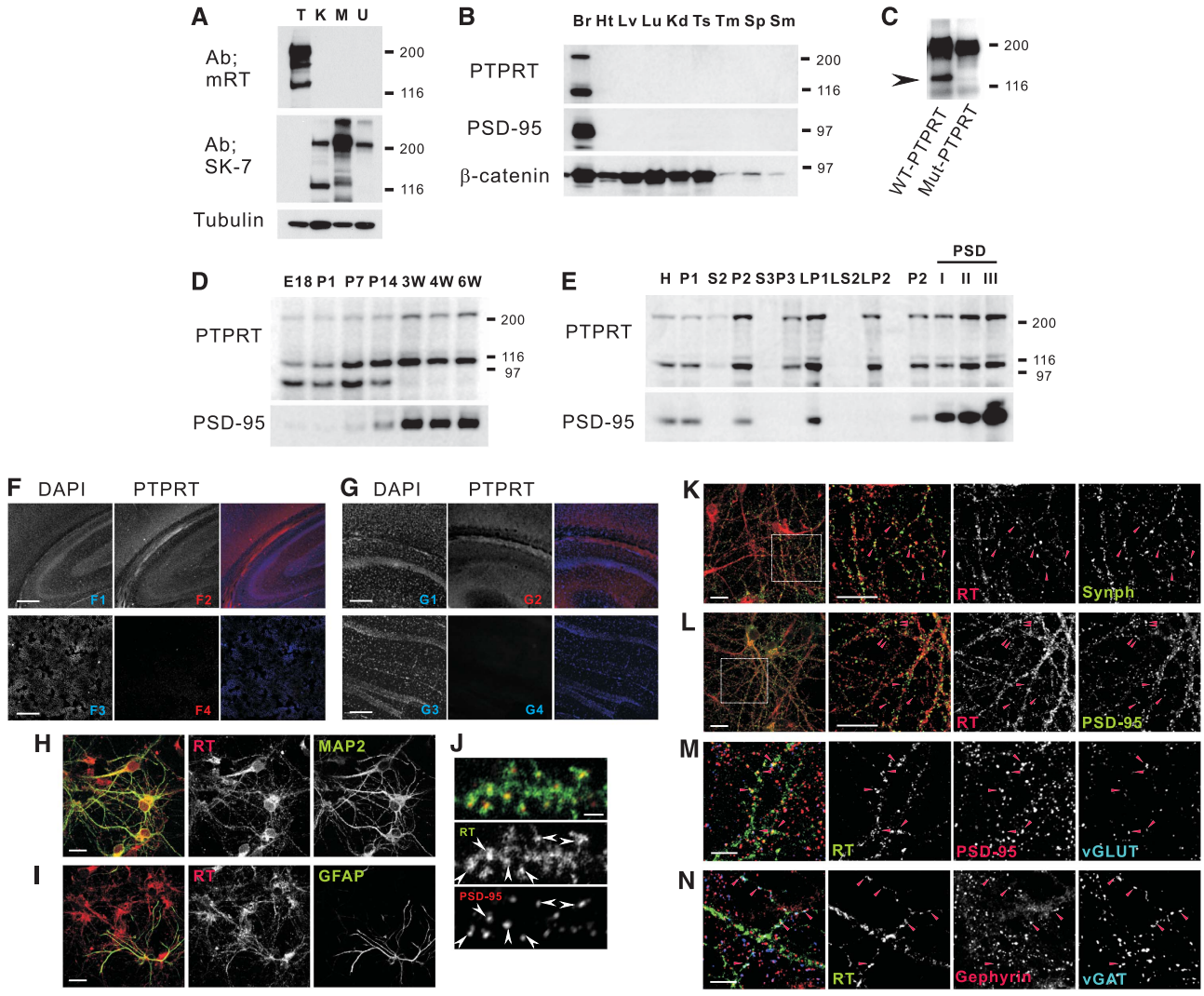

Figure 1 PTPRT localizes only to the brain and neuronal synapses. (**A**) The specificity of PTPRT monoclonal antibody was evaluated by immunoblotting of each PTPRT(T), PTPRK(K), PTPRM(M), and PTPRU(U), respectively, overexpressed in heterologous cells. PTPRT-specific monoclonal antibody (mRT) recognized only PTPRT and did not PTPRK, PTPRM, PTPRU that were detected by antibody SK-7 (generously gifted by Dr Brady-Kalnay). (**B**) Tissue distribution patterns of PTPRT revealed by immunoblot analysis. Monoclonal antibodies specific for PTPRT (Supplementary Figures S1A and B) were used. Br, brain; Ht, heart; Lv, liver; Lu, lung; Kd, kidney; Ts, testis; Tm, thymus; Sp, spleen; Sm, skeletal muscle. PSD-95 and β-catenin were used as controls. (**C**) The short form of PTPRT was generated by furin protease. The short form (indicated by an arrowhead) disappeared by the mutation of the predicted furin-cleavage site (KSRR→NSLR). (**D**) Developmental pattern of PTPRT in the rat brain. E, embryonic; P, postnatal days. PSD-95 was used as a control. (**E**) Distribution pattern of PTPRT in biochemical rat brain fractions. PTPRT is retained in the PSD III fraction. H, homogenate; P1, cell and nuclei-enriched pellet; P2, crude synaptosomes; S2, supernatant after P2 precipitation; S3, cytosol; P3, light membranes; LP1, synaptosomal membranes; LS2, synaptosomal cytosol; LP2, synaptic vesicle-enriched fraction (see Materials and methods). PSD-95 was used as a control. (**F**) In brain slices, PTPRT monoclonal antibodies revealed PTPRT expression in specific brain regions (F2), whereas signals could not be detectable in the kidney (F4). F1&3, DAPI signal; F2&4. F1&2, rat brain; F3&4, rat kidney. Scale bar, 1 mm. (**G**) As pre-incubated with cognate antigen proteins, PTPRT signals disappeared in brain slices. G1&3, DAPI signal; G2&4, PTPRT. G1&2, original antibody; G3&4, pre-incubated antibody. Scale bar, 0.5 mm. (**H**, **I**) Expression patterns of PTPRT in rat neurons stained with MAP2 and in rat astrocytes stained with GFAP. Scale bar, 20 μm. (**J**) PTPRT was localized to the dendritic spines marked with PSD-95 (arrowhead). Scale bar, 2 μm. (**K**, **L**) PTPRT co-localized to neuronal synapses stained with synaptophysin and PSD-95. Scale bar, 20 μm. (**M**, **N**) EGFP-tagged PTPRT co-localized to excitatory synapses with PSD-95 and vGLUT or to inhibitory synapses with gephyrin and vGAT. Scale bar, 10 μm.

dendritic spines resulting from the overexpression of WT PTPRT (WT-RT) significantly increased compared with control neurons (Figure 2A; Supplementary Figure S2A). In the case of the activity-dead mutant (2cs-RT), the spine density was less than that of WT-RT, but was not reduced to the control level, suggesting that some interaction partner recruitment occurred through the ecto-domain or the endogenous substrate was trapped to 2cs-RT (Barford *et al*, 1995). In some cases WT and the activity-dead mutant PTP show similar phenotypes because both of them could block signal transductions by dephosphorylating (WT) or trapping (the activity-dead mutant) substrates. However, the spine length of dendrites in these mutants was greater, indicating immature synapse formation because of the elimination of PTP activity (below, Supplementary Figure S2B). The distributions of the representative synaptic markers were examined

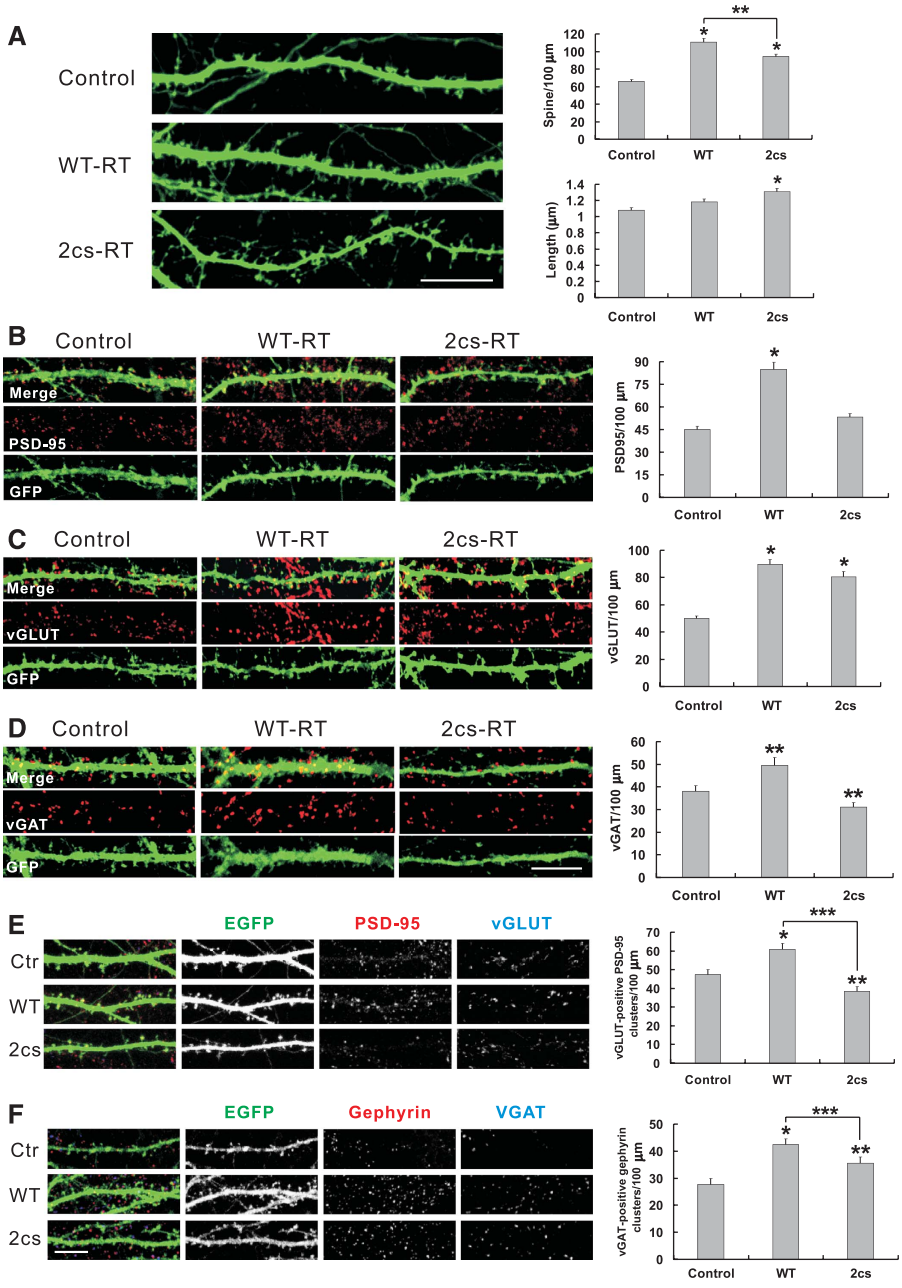

Figure 2 Enhanced synapse formation by overexpression of PTPRT. (**A**) Increased spine density by PTPRT. Cultured hippocampal neurons were transfected at DIV9 with pSuper.gfp/neo only (control) or with PTPRT (WT-RT, 2cs-RT), and immunostained for GFP at DIV 20 (Supplementary Figure S2A). When wild-type PTPRT (WT-RT) was overexpressed, the density of dendritic spines increased compared with the control. In the case of the PTPRT activity-dead mutant (2cs-RT), the increase of spine density was less than WT although spine density increased compared with the control. Mean ± s.e.m. $n = 51$ dendrites for control, 37 for WT-RT, and 36 for 2cs-RT. $^{*}P < 0.0001$ and $^{**}P < 0.005$ (Student's *t*-test). Scale bar, 10 μm. (**B–F**) Enhanced synapse formation by PTPRT. After transfection at DIV9, the cultured neurons were immunostained for GFP (green) and PSD-95, vGLUT, or vGAT (red). PTPRT expression increased the number of synaptic markers. (B) PSD-95 staining. Mean ± s.e.m. $n = 49$ dendrites for control, 50 for WT-RT, and 53 for 2cs-RT. (C) vGLUT staining. Mean ± s.e.m. $n = 32$ dendrites for control, 42 for WT-RT, and 43 for 2cs-RT. (D) vGAT staining. Mean ± s.e.m. $n = 55$ dendrites for control, 31 for WT-RT, and 33 for 2cs-RT. $^{*}P < 0.0001$ and $^{**}P < 0.01$ (Student's *t*-test). Scale bar, 10 μm. (E) The number of excitatory synapses (vGLUT-positive PSD-95 clusters). Mean ± s.e.m. $n = 30$ dendrites for control, 31 for WT-RT, and 30 for 2cs-RT. $^{*}P = 0.0017$, $^{**}P = 0.0205$, and $^{***}P < 0.0001$ (Student's *t*-test). Scale bar, 10 μm. (F) The number of inhibitory synapses (vGAT-positive gephyrin clusters). Mean ± s.e.m. $n = 27$ dendrites for control, 28 for WT-RT, and 28 for 2cs-RT. $^{*}P < 0.0001$, $^{**}P = 0.0176$, and $^{***}P = 0.0346$ (Student's *t*-test). Scale bar, 10 μm.

to obtain more evidence to support the role of PTPRT in synapse formation (Figure 2B–D). The density of PSD-95 increased with transfection of WT-RT but not with transfection of 2cs-RT compared with the control (Figure 2B). Many areas in which increased spines were induced by 2cs-RT expression did not appear to be real synapses; therefore, PTP activity is necessary for mature synapse formation (Supplementary Figure S2B). The density of vGLUT was increased by WT-RT and considerably increased by 2cs-RT (Figure 2C). The density of vGAT was increased by WT-RT and not by 2cs-RT (Figure 2D). To verify the excitatory synapse formation vGLUT-positive PSD-95 clusters were examined

(Figure 2E). When PTPRT was overexpressed, the excitatory synapses were increased. When vGAT-positive gephyrin clusters were examined, the inhibitory synapses were also increased by overexpression of PTPRT (Figure 2F).

Synapse formation is inhibited by knockdown of PTPRT

To inhibit PTPRT expression in cultured neurons, specific short-interfering RNA (siRNA) (RTsiRNA#1) was produced in the pSuper.gfp/neo vector and the effects of PTPRT knockdown on synapse formation were examined (Supplementary Figure S2C). Spine density was dramatically decreased by PTPRT knockdown and somewhat rescued by the overexpression of PTPRT (Resc RT) (Figure 3A). However, the rescued spine morphology did not appear as mature as the control, which suggests that the effects of PTPRT knockdown by siRNA are irreversible. Knockdown of PTPRT caused PSD-95 puncta to significantly decrease (Figure 3B), and density of vGLUT and vGAT was attenuated (Figure 3C and D). To verify the effect of PTPRT knockdown new siRNA (RTsiRNA#2) was produced and synapse formation was examined (Supplementary Figure S2D). Spine density was decreased by PTPRT knockdown and rescued by the overexpression of PTPRT (Figure 3E). Contrary to former siRNA the rescued spine morphology was as mature as the control. The frequency of mEPSC was reduced dramatically, but not the amplitude by PTPRT knockdown in cultured neurons (Figure 3F). These results confirm that PTPRT regulates synapse formation in hippocampal neurons.

PTPRT interacts with neuroligin and neurexin through its extracellular ecto-domain

Rat brain synaptosomal fractions extracted with sodium deoxycholate were immunoprecipitated with anti-PTPRT monoclonal antibody to determine the identity of endogenous PTPRT interaction partners. Co-precipitants were resolved by SDS–PAGE, then the proteins in ~50 gel pieces were digested with trypsin and identified by tandem mass spectrometry (Figure 4A) (Husi *et al*, 2000). Among the candidates of interaction partners, neuroligin 3 was identified by two peptides (Figure 4B). The amino acid sequences of these peptides were conserved in all neuroligins (NLG1,2,&3) except for one amino acid. PTPRT associates with neuroligin and neurexin in the brain synaptosome (Figure 4C). When immunoprecipitation was performed using an anti-PTPRT monoclonal antibody, neuroligin and neurexin co-precipitated with PTPRT. As neuroligin and neurexin are receptors of each other in the synapse, the co-precipitated neurexin was considered a reasonable result. Conversely, PTPRT and neuroligin were co-precipitated using anti-neurexin-specific antibody (Figure 4C; Supplementary Figure S1C). The interactions between PTPRT and neuroligin or neurexin were investigated through co-immunoprecipitation in heterologous cells (Supplementary Figures S3 and S4). PTPRT seems to associate with members of the neuroligin and neurexin families with varying intensity.

To define the domains of PTPRT that interact with neuroligin and neurexin, several PTPRT truncation mutants were tested in heterologous cells (Figure 4D; Supplementary Figure S5). Only full-length PTPRT co-precipitated with neuroligin and neurexin, whereas truncated PTPRT without the extracellular ecto-domain did not (Figure 4E). Only ecto-domain of PTPRT without intracellular domains (ΔJDD&ΔDD) was sufficient for co-immunoprecipitation with neuroligin and neurexin even though neurexin seems to interact with PTPRT in somewhat different ways from neuroligin (Figure 4F; Supplementary Figure S6). PTPRT seemed to interact with neuroligin and neurexin through extracellular ecto-domains. In cultured neurons, PTPRT and neuroligin were co-localized as much as neuroligin and PSD-95 (Figure 4G, arrowhead). On the basis of these results, PTPRT seems to associate with neuroligin and neurexin in the pre- and post synapse.

PTPRT interacts with neuroligin and neurexin functionally

The expression level of neuroligin was examined in cultured neurons when PTPRT was overexpressed. The numbers of neuroligin1 and neuroligin2 puncta was increased by overexpression of WT PTPRT, which suggests that PTPRT recruited synaptic neuroligin (Figure 5A and B). To analyse whether the synapse-inducing activity of neuroligin is regulated by PTPRT, the density of dendritic spine was examined when neuroligin was overexpressed in the same neurons that the expression of PTPRT was inhibited by siRNA (Figure 5C). The synaptic formation induced by neuroligin seemed to be attenuated by PTPRT knockdown whereas neuroligin functioned normally in cultured neurons that still expressed PTPRT as reported earlier (Chih *et al*, 2005). Soluble PTPRT ecto-Fc was produced in heterologous cells, and purified PTPRT ecto-Fc was incubated with the hippocampal primary cultured neurons. After several days, the density of dendritic spines and the synapsin puncta was significantly decreased compared with control cells (Figure 5D).

To define the main cause of inhibition, a pull-down assay using purified PTPRT ecto-Fc 'pre-bound' on protein A-beads was performed (Figure 5E). It was hypothesized that the *trans*-interactions could be shown mainly in this scheme because the streric hindrances from pre-bound protein A-bead inhibit the *cis*-interaction. Interestingly, the interactions between the ecto-domains of PTPRT and neuroligins/neurexins were not as strong as the PTPRT homophilic interactions. Next purified PTPRT ecto-Fc was mixed with neuroligin before addition of protein A-beads and significant neuroligins were pulled down (Figure 5F). These results suggest that the interactions between PTPRT and the cell adhesion molecules could be a *cis*-interaction rather than a *trans*-interaction. To confirm *cis*-interaction between PTPRT and cell adhesion molecules, PTPRT ecto-Fc was co-expressed with cell adhesion molecules in heterologous cells and then a pull-down assay was performed in the cell lysate (Figure 5G). This time, neuroligin and neurexin were pulled down by PTPRT ecto-Fc proteins suggesting *cis*-interaction between PTPRT and cell adhesion molecules.

Tyrosine phosphorylation of PTPRT by Fyn attenuates synapse formation

Phospho-tyrosine levels are regulated through PTP–PTK interactions in the cell, and PTP could be a substrate for PTK, and hence the functions of PTP could potentially be regulated by tyrosine phosphorylation. The phospho-tyrosine level of PTPRT was examined in cultured neurons treated with pervanadate, a potent phospho-tyrosine phosphatase inhibitor, and PTPRT was shown to be phosphorylated at tyrosine residues (Figure 6A). Of several possible PTK candidates responsible for tyrosine phosphorylation of PTPRT, Fyn

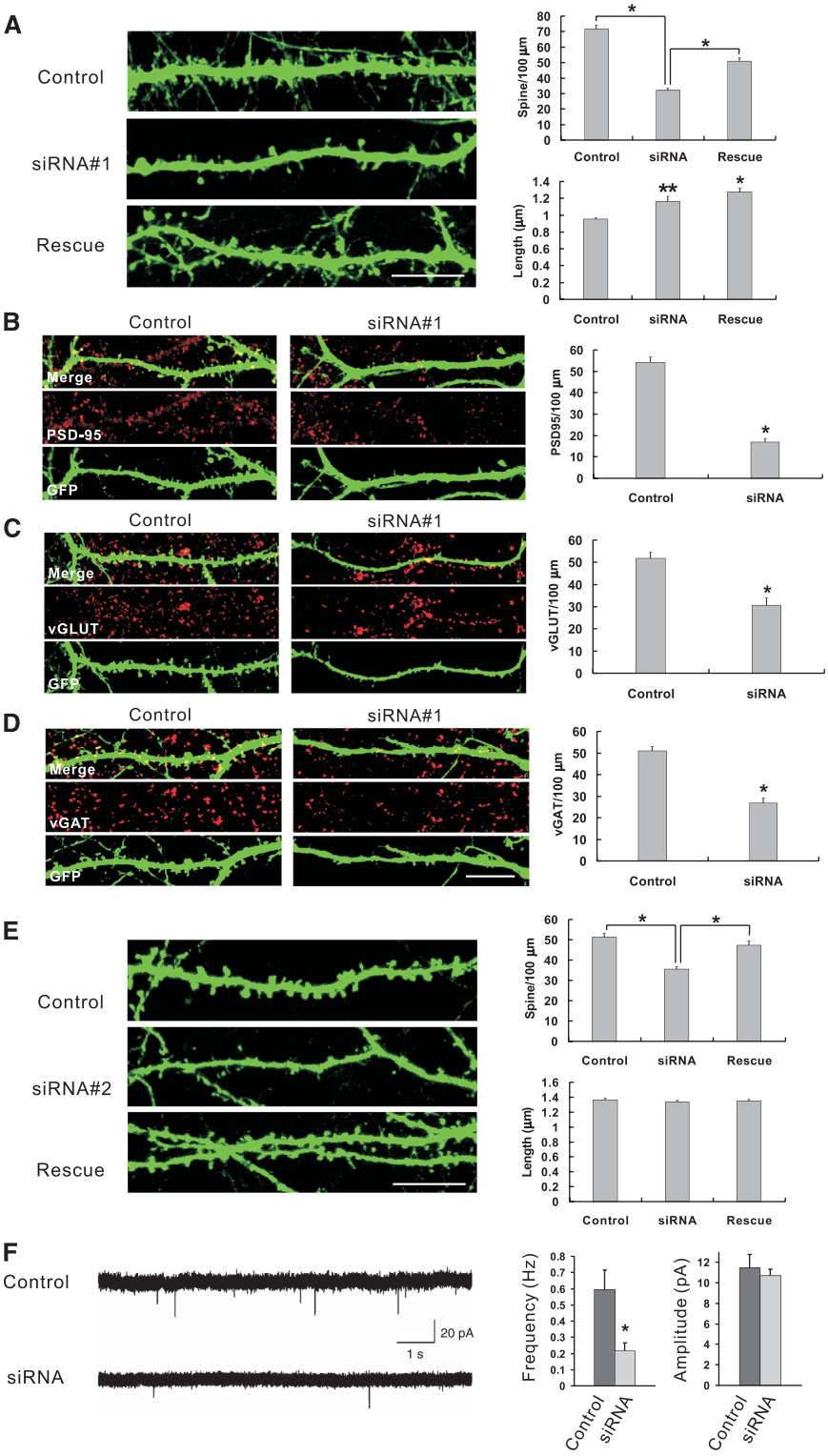

Figure 3 Loss of synapses by knockdown of PTPRT. (**A**) PTPRT knockdown using siRNA (RTsiRNA#1) reduced the spine density and was rescued by overexpression of PTPRT (Supplementary Figure S2C). Mean ± s.e.m. $n = 55$ dendrites for control (pSuper.gfp/neo), 69 for siRNA, and 65 for rescue. $^*P < 0.0001$, $^{**}P < 0.005$ (Student's *t*-test). Scale bar, 10 μm. (**B–F**) Reduced synapse formation by knockdown of PTPRT. The synaptic markers PSD-95, vGLUT, and vGAT showed decreased synapse formation when PTPRT was knocked down. (B) PSD-95 staining. Mean ± s.e.m. $n = 36$ dendrites for control and 32 for siRNA. (C) vGLUT staining. Mean ± s.e.m. $n = 40$ dendrites for control and 30 for siRNA. (D) vGAT staining. Mean ± s.e.m. $n = 40$ dendrites for control and 32 for siRNA. $^*P < 0.0001$ (Student's *t*-test). Scale bar, 10 μm. (E) PTPRT knockdown using new siRNA (RTsiRNA#2) reduced the spine density and was rescued by overexpressing PTPRT (Supplementary Figure S2D). Mean ± s.e.m. $n = 31$ dendrites for control, 32 for siRNA, and for 28 rescue. $^*P < 0.0001$ (Student's *t*-test). Scale bar, 10 μm. (F) Knockdown of PTPRT in cultured neurons (DIV 13–16) decreased the frequency, but not amplitude of mEPSCs ($n = 12$ for control and $n = 10$ for siRNA, $^*P = 0.015$, Student's *t*-test).

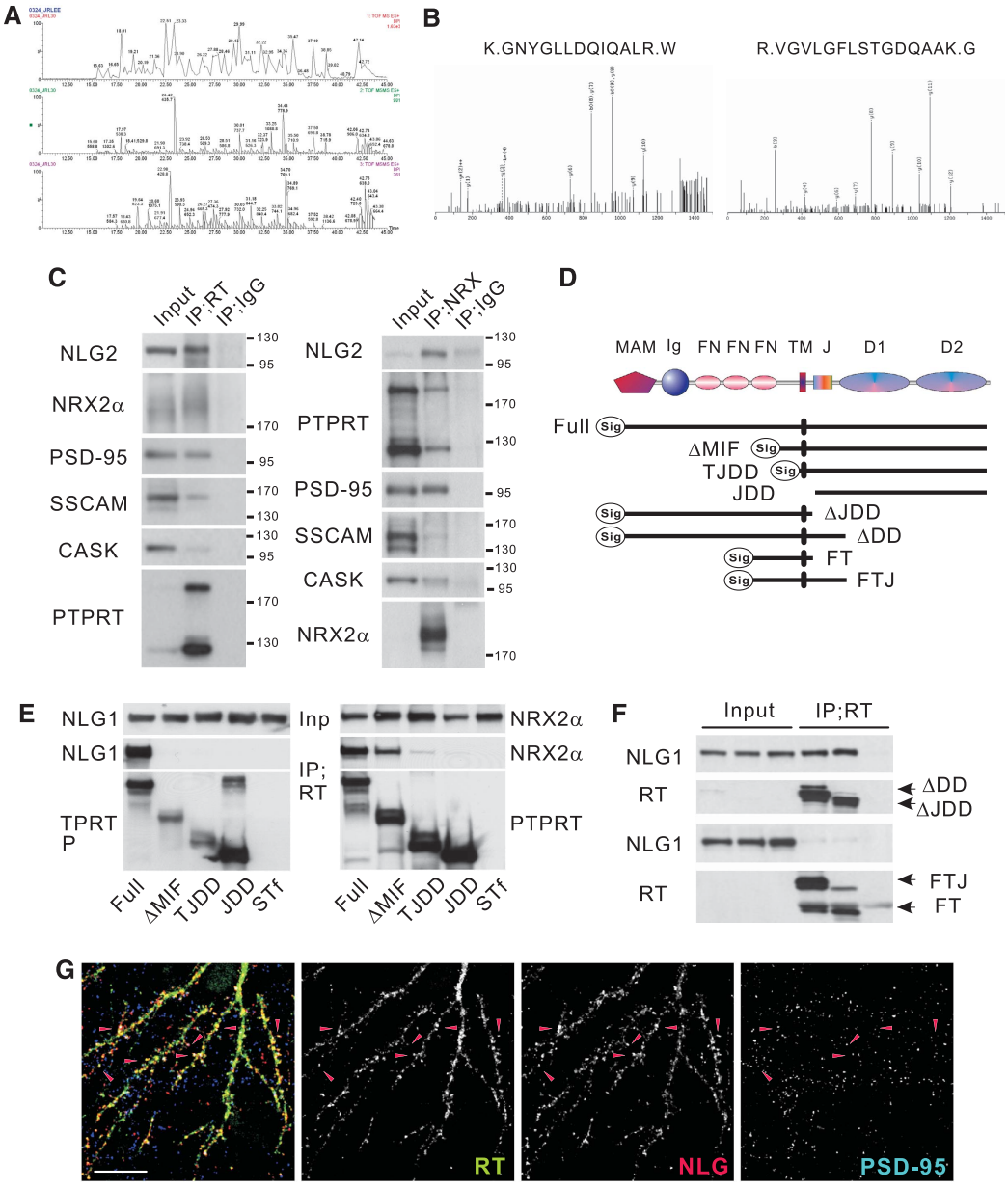

Figure 4 Interaction of PTPRT with neuroligin and neurexin. (**A**) Representative base peak chromatograms generated in MS and MS/MS modes. The example given shows the trypsin digestion products of 30th SDS-gel bands corresponding to a ~100 kDa protein band. The top panel shows the base peak chromatogram of the MS survey scan, and the lower two panels are the base peak chromatogram of MS/MS channels. (**B**) Combined MS/MS spectra of neuroligin 3 peptide ions. The amino acid sequences were identified using the Mascot database search program. The matched fragment ion peaks for the most probable sequence are labelled on the spectra. (**C**) *In vivo* co-immunoprecipitation in the rat brain synaptosome. Neuroligin 2 and neurexin 2α were co-precipitated by treatment with PTPRT monoclonal antibody. PTPRT also was co-precipitated by specific antibody for neurexin 2α (Supplementary Figure S1C). Input, 10%. Quantification; (left column) NLG, 126; NRX2α, 153; PSD-95, 61.9; SSCAM, 19.4; CASK, 10.4; PTPRT, 601; (right column) NLG, 386; PTPRT, 23.6; PSD-95, 77.5; SSCAM, 12.7; CASK, 61.5; NRX2α, 883 (%, immunoprecipitated/input proteins). (**D**) Domain structure of PTPRT and the deletion mutants used for *in vitro* co-immunoprecipitation. Signal peptides were added to the N-terminus of all expression constructs except JDD. MAM, Meprin/A5/PTPmu domain; Ig, immunoglobulin-like domain; FN, fibronectin-type III-like domain; TM, trans-membrane domain; J, juxta-membrane domain; D1 and D2, PTP-catalytic domains. (**E**) Co-immunoprecipitation using a deletion mutant of PTPRT without the extracellular ecto-domain in the heterologous cells. PTPRT interacts with neuroligin and neurexin through PTPRT's ecto-domain. Note that neurexin 2α showed a different interaction pattern with ΔMIF than neuroligin. STf, single transfection; Inp, input (Supplementary Figures S3 and S4). Input, 3%. (**F**) The interaction of PTPRT ecto-domains with neuroligin. Neuroligin 1 was recruited by PTPRT ecto-domain mutants (Supplementary Figure S5). Input, 3%. (**G**) Co-localization of PTPRT and neuroligin 2. Overexpressed PTPRT and neuroligin 2 were co-localized in cultured hippocampal neurons (arrowhead). Scale bar, 20 μm.

PTK was examined because Src-related PTKs were discovered as interactive factor from IP-proteomics (data not shown). When the constitutively active form of Fyn PTK (caFyn) (Liu *et al*, 2006) was co-expressed in heterologous cells with PTPRT, Fyn was recruited to PTPRT and tyrosine residues of PTPRT were phosphorylated (Figure 6B). On the other hand, PTPRT was not phosphorylated when co-transfected with kinase-dead mutant of Fyn (kdFyn). WT-RT seems to be

auto-dephosphorylated, and the phospho-tyrosine level of WT-RT was lower than that of the activity-dead mutants (csRT and 2csRT). Then two tyrosine residues (Y912, Y1027) in the first catalytic domain of PTPRT, predicted to be candidates for phosphorylation by Fyn PTK, were changed to phenylalanine for phospho-tyrosine immunoblotting (Figure 6C). As the phospho-tyrosine residues of WT-RT underwent auto-dephosphorylation, YF mutants were constructed in the activity-dead PTPRT context (2csRT). The level of tyrosine phosphorylation was significantly decreased in the Y912F mutant compared with single 2cs and the Y1027F mutant although not decreased to the 2YF mutant, therefore the 912 tyrosine residue seems to be the major target of Fyn PTK.

To determine the effects of Fyn PTK on the synapse formation activity of PTPRT, caFyn PTK was co-expressed with PTPRT in cultured neurons (Figure 6D). PTPRT-mediated synapse formation was attenuated by caFyn PTK, which suggests that Fyn PTK regulates the function of PTPRT through tyrosine phosphorylation during synapse formation, but expression of Fyn alone had no effect on synapse formation in this system (Supplementary Figure S7A). To confirm the 912 tyrosine residue is the major target of Fyn; the density of dendritic spine was examined when YF mutants were co-expressed with Fyn (Supplementary Figure S7B). Y912F mutant still increased the number of dendritic spine, but WT and Y1027F mutant did not when Fyn was co-expressed. The Fyn-targeted tyrosine residue was changed to a glutamate residue to mimic a phosphate group, and then the effect of this mutation on synapse formation was examined by overexpressing Y912E-RT in cultured neurons (Figure 6E). As expected, synapse formation by overexpression of PTPRT was attenuated when tyrosine 912, but not tyrosine 1027, was mutated to glutamate (Supplementary Figure S7C). When tyrosine residues were changed to phenylalanine to block phosphorylation, synapse formation was induced as much as in WT (Supplementary Figure S7C). From these results, we suggest that tyrosine residue 912 is a major target of Fyn and synapse formation can be regulated by phosphorylation of this residue.

PTPRT activity and the PTPRT–neuroligin interaction are regulated by Fyn

To elucidate the regulatory effect of tyrosine phosphorylation on PTPRT-induced synapse formation, an *in vitro* PTP assay was first carried out using recombinant proteins. PTP activity was remarkably reduced when the Y912E mutation was introduced, but not when the Y1027E mutation was introduced (Figure 7A). Therefore, Fyn seems to regulate PTPRT activity by phosphorylating specific tyrosine residue in PTPRT's catalytic domain.

The effects of tyrosine phosphorylation on the homophilic interactions of PTPRT were then examined, because *cis*-homophilic interactions of PTPRT were suggested in the PTPRT ecto-Fc experiment (Figure 5F and G) and it is possible that an inactive *cis*-dimer of PTPRT may exist, as seen for RPTPα (Blanchetot *et al*, 2002). Although considerable PTPRT seemed to compose dimer already, Fyn was shown to reinforce the homophilic interaction of PTPRT in experiments using differentially tagged PTPRT (Figure 7B). The effects of tyrosine phosphoryaltion on homophilic interaction of PTPRT were examined in cultured neurons (Figure 7C). The clustering of PTPRT could be reflected by puncta of PTPRT in cultured neurons even though the possible difference between molecular and cellular phenomena cannot be ruled out. The area and intensity of PTPRT-EGFP puncta were increased by overexpression of Fyn whereas the number of PTPRT-EGFP puncta was decreased significantly. To know effects of PTPRT clustering on synaptic localization, co-localizations of PTPRT and neuroligin were evaluated (Figure 7D). When Fyn was co-expressed, less neuroligin puncta were found to be with PTPRT and it seems to be related with attenuated synapse formation.

Homophilic multimerization—possibly *cis*-interaction seems to decrease PTPRT activity and as a result synapse formations could become attenuated by uncontrollable phosphorylation of synaptic substrates (Supplementary Figure S9). Dimerization of PTPRT could be enhanced by PTPRT ecto-Fc in reduced synapse formation because Fc-fusion proteins compose dimer (Figure 5D). Inactivated PTPRT clusters might deform neuronal synapses and appear to be far from neuroligin. Thus, Fyn PTK induces multimerization and inactivation of PTPRT by phosphorylating tyrosine residue 912 in the catalytic domain resulting in the attenuation of synapse formation.

Discussion

PTPRT regulates synapse formation by gaining access to synaptic substrates connected with cell adhesion molecules, and its activity seems to be regulated through tyrosine phosphorylation by Fyn PTK. Inactivated PTPRT could not control synaptic substrates nor induce synapse formation.

The modelling of PTPRT catalytic domain

The 912 tyrosine residue seems to be the major target of Fyn and the homophilic interaction of PTPRT was induced by Fyn (Figures 6C and 7B). On the basis of these results and a model for dimerization of RPTPα, one hypothesis in the structural context of PTPRT was developed (Bilwes *et al*, 1996). In the model of RPTPα, a wedge formed by helix(α1′)-turn-helix(α2′) segment at the N-terminus of one monomer occludes the catalytic face of the other monomer within dimer, which would completely block the access of the substrates (Supplementary Figure S8). Tyrosine 912 of PTPRT belongs to helix α2′ of wedge and is situated in the interface between wedge and the body of the catalytic domain. In the crystal structure of PTPRK/RPTPκ (pdb code: 2c7s), tyrosine 892, equivalent to tyrosine 912 in PTPRT, participates in extensive hydrogen-bonding interaction (Figure 7E) (Eswaran *et al*, 2006). The phosphorylation of 892 would result in the clashes with the surrounding residues and the detachment of the wedge from the body of the catalytic domain. The resulting flexible wedge may enter the catalytic pocket of other monomer deeply, strengthen the dimeric interaction, and eventually inhibit catalytic activity.

Thus, Fyn PTK might induce *cis*-multimerization and inactivation of PTPRT by phosphorylating tyrosine residue 912 in the wedge of the catalytic domain resulting in the attenuation of synapse formation.

The regulation of synapse formation by PTPRT and Fyn PTK

There have been many reports that PTK activity is regulated through dephosphorylation by PTP. CD45 PTP is thought to dephosphorylate the non-receptor Lck PTK, thereby enhancing PTK signal transduction activity (Mustelin and Altman, 1990). RPTPα regulates Fyn activity through interaction with NCAM and the elongation of neurites (Bodrikov *et al*, 2005). RPTP LAR was also suggested to regulate Lck and Fyn PTK activity, although no linker between LAR and PTK has been discovered to date (Tsujikawa *et al*, 2002). PTPRO functions in negative regulation of the Eph receptor tyrosine kinase in retinal axon growth (Shintani *et al*, 2006). Conversely, examples of PTK controlling the activity of PTP through tyrosine phosphorylation have been suggested in several cases such as PTP D1 and RPTPα (Vogel *et al*, 1993; Zheng *et al*, 2000).

Here, PTPRT seems to be regulated by Fyn PTK through tyrosine phosphorylation. The catalytic activity of PTPRT was decreased to basal levels through phosphorylation of a specific tyrosine (Y912) by Fyn. PTPRT seems to be connected to its substrates through neuroligin and neurexin, well-known

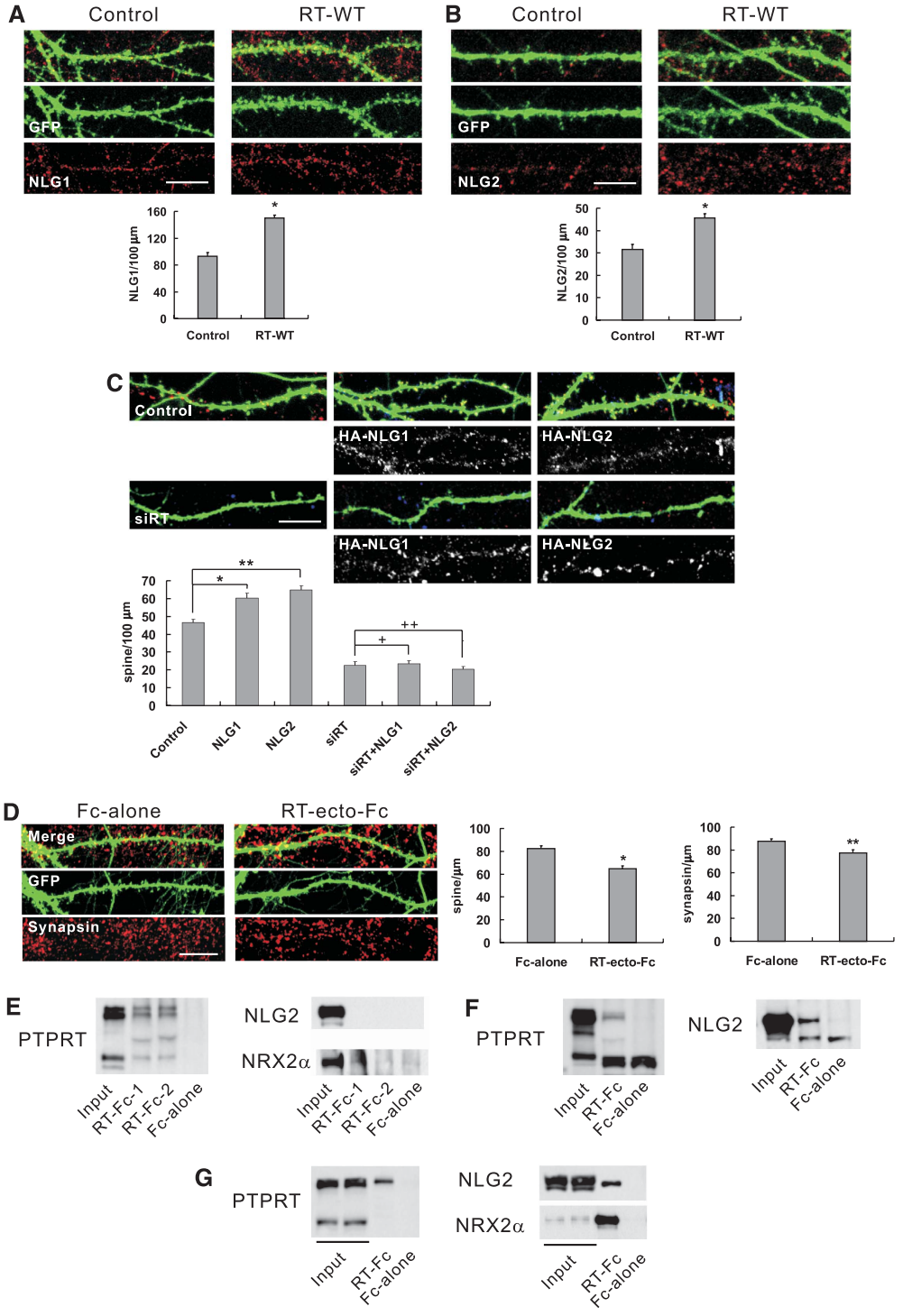

synaptic molecules inducing synapse formation. When PTPRT activity is attenuated by phosphorylation by Fyn, the functions of synaptic molecules may be impaired by hyper-phosphorylation. In our system, overexpression of Fyn alone did not induce a significant increase in synapse formation (Supplementary Figure S7A). Although hyper-phosphorylation of synaptic molecules by Fyn itself could not be completely ruled out, inactivation of PTPRT through tyrosine phosphorylation by Fyn could account for the attenuation of synapse formation by Fyn.

As PTPRT seems to be auto-dephosphorylated, the level of phosphorylation in the YF mutant was not significantly different from that of non-YF mutant in a WT background (WT-RT, data not shown). To visualize contrasts of phosphorylations, we constructed a YF mutant in the activity-dead mutant (2csRT, Figure 6C). It is possible that Fyn PTK could be a substrate of PTPRT, because the phospho-tyrosine level of WT Fyn was somewhat decreased by WT-PTPRT (data not shown). PTP and PTK could therefore be substrates of one another, and their activities could be fine regulated by phospho-tyrosine levels in the neurons. Neuroligin and neurexin do not seem to be substrates of Fyn or PTPRT, because no phospho-tyrosine forms of these proteins were detected in neuronal samples. However, it is possible that a rapid reaction results in no detectable neuroligin or neurexin phospho-tyrosine residues.

Roles of the interaction between PTPRT and cell adhesion molecules

The ecto-domains of full-length proteins seem to facilitate *trans*-homophilic interactions although PTPRT, PTPRM, and PTPRK are partially processed. PTPRM has been demonstrated to interact with E-cadherin through its intracellular domain (Brady-Kalnay *et al*, 1995). PTPRT has also been reported to interact with cadherins and catenins through intracellular domains (Besco *et al*, 2006). However, STAT3, a substrate candidate of PTPRT, was found by using only the extracellular portion of PTPRT expressed in HEK293T cells (Zhang *et al*, 2007). It is therefore necessary to examine the function of RPTPs through ecto-domain interactions. In this study, neuroligin was identified as a protein that interacts with PTPRT through immunoprecipitation and mass spectrometry. Experiments using various truncations showed that the ecto-domain of PTPRT is responsible for its interaction with neuroligin. PTPRT also showed *trans*-homophilic interactions, similar to PTPRM and PTPRK, in experiments using ecto-Fc recombinant proteins (Figure 5E) (Aricescu *et al*, 2007). This raises the question as to how PTPRT interacts with cell adhesion molecules. Cell adhesion molecules are generally considered to act by clustering and are thought not to function properly as single molecules. However, X-ray scattering and neutron contrast variation data revealed that two neurexin monomers bind at symmetric locations on opposite sides of the long axis of the neuroligin dimer (Arac *et al*, 2007; Comoletti *et al*, 2007). PTPRT could interact with neuroligin and neurexin in a *cis*-manner and consolidate the interaction between neuroligin and neurexin by adding its homophilic *trans*-interaction. If PTPRT is a component of the cell adhesion molecule cluster, the homophilic interaction of PTPRT could have a key function in cell adhesion molecule cluster function. The number of neuroligin puncta was increased by overexpression of PTPRT and synapse formation induced by neuroligin was attenuated by knockdown of PTPRT (Figure 5A–C). These results suggested PTPRT and neuroligin are functionally connected with each other for synapse formation in the neuronal synapses. Interestingly, PTPRT seems to make *cis*-homophilic interactions in addition to *trans*-homophilic interactions, and these *cis*-homophilic interactions seem to be reinforced by Fyn (Figures 5G and 7B). Sequentially, decreased PTP activity could result in failure in dephosphorylation of various neuronal substrates and could not consolidate neuronal synapses, and *cis*-multimerized PTPRT seems to collapse neuronal synapses and be dissociated from neuroligin (Figure 7D). The *cis*-interaction between PTPRT and neuroligin or neurexin could make substrates linked to cell adhesion molecules accessible to PTPRT for consolidation of synapse formation. When PTPRT was knocked down in cultured neurons, dephosphorylation might be not regulated, resulting in severe synapse depletion.

Neuronal disease related to PTPRT

Mutations in two X-linked genes encoding neuroligins 3 and 4 were found in the brains of siblings with autism-spectrum disorders (Jamain *et al*, 2003). As synapse formation is

Figure 5 PTPRT interacts with neuroligin and neurexin functionally. (**A**) PTPRT increases neuroligin1 puncta. Cultured hippocampal neurons were transfected at DIV8 with pSuper.gfp/neo only (control) or with wild-type PTPRT (WT-RT), and immunostained for GFP at DIV15. When WT PTPRT (WT-RT) was overexpressed, the number of neuroligin1 puncta increased compared with the control. Mean ± s.e.m. $n=24$ dendrites for control, 26 for WT-RT. $^{*}P<0.0001$ (Student's *t*-test). Scale bar, 10 μm. (**B**) PTPRT increases neuroligin2 puncta. By WT PTPRT (WT-RT) overexpression the number of neuroligin2 puncta increased compared with the control. Mean ± s.e.m. $n=23$ dendrites for control, 28 for WT-RT. $^{*}P<0.0001$ (Student's *t*-test). Scale bar, 10 μm. (**C**) Synaptic formation induced by neuroligin was prevented by knockdown of PTPRT. Cultured hippocampal neurons were transfected at DIV10 with HA-tagged neuroligins (HA-NLG) with or without siRNA of PTPRT (siRT) and stained for GFP and HA at DIV17. The number of dendritic spine was not increased by overexpression of neuroligin in the same neuron transfected with siRNA of PTPRT. Mean ± s.e.m. $n=36$ dendrites for control, 34 for HA-NLG1, 36 for HA-NLG2, 34 for siRT, 26 for siRT, and HA-NLG1, 23 for siRT and HA-NLG2. $^{*}P=0.0002$, $^{**}P<0.0001$, $^{+}P=0.7527$, and $^{++}P=0.4291$ (Student's *t*-test). Scale bar, 10 μm. (**D**) Cultured hippocampal neurons transfected with pSuper.gfp/neo to visualize dendritic spines (DIV9–20) were incubated with PTPRT-ecto-Fc-fusion proteins, or Fc alone (control), for 5 days (DIV15–20) and stained for GFP and synapsin. PTPRT-ecto-Fc reduced the number of dendritic spines and synapsin-antibody stained synapses. Mean ± s.e.m. $n=48$ dendrites for Fc-alone and 42 for RT-ecto-Fc. $^{*}P<0.0001$ and $^{**}P<0.01$ (Student's *t*-test). Scale bar, 10 μm. (**E**) PTPRT expressed in heterologous cells was recruited by the PTPRT-ecto fusion proteins; purified RT-Fc-1 (aa 1–749) and RT-Fc-2 (aa 1–763) pre-bound to the protein A-agarose beads. However, neuroligin and neurexin were recruited to a lesser extent than PTPRT. Input, 3%. (**F**) Protein A-beads were added after purified PTPRT-ecto-Fc and neuroligin expressed in heterologous cells were mixed. PTPRT and neuroligin were recruited to PTPRT-ecto-Fc. Input, 2%. (**G**) PTPRT, neuroligin, and neurexin were expressed with PTPRT-ecto-Fc in heterologous cells and cell lysate without cell media was used for pull-down assay. When PTPRT-ecto-Fc was pulled down by protein A-agarose beads, PTPRT, neuroligin, and neurexin were recruited to PTPRT-ecto-Fc. Input, 3%.

regulated by the interaction of PTPRT with neuroligin, and because many PTPRT mutations have been reported in colon cancer (Wang *et al*, 2004), defining the relationship between neuronal diseases and the PTPRT gene would be of significant interest. PTPRT and Fyn kinase could be a possible drug targets for neuronal disease treatment.

Materials and methods

DNA constructs

Full-length human PTPRT (NM_133170, aa 1–1460; from a human brain cDNA library; Clontech) was subcloned into GW1-CMV. For FLAG tagging the N-terminus, a 3xFLAG epitope (MDYKDHDG-DYKDHDIDYKDDDDK; p3xFLAG-CMV-7.1, Sigma) was inserted

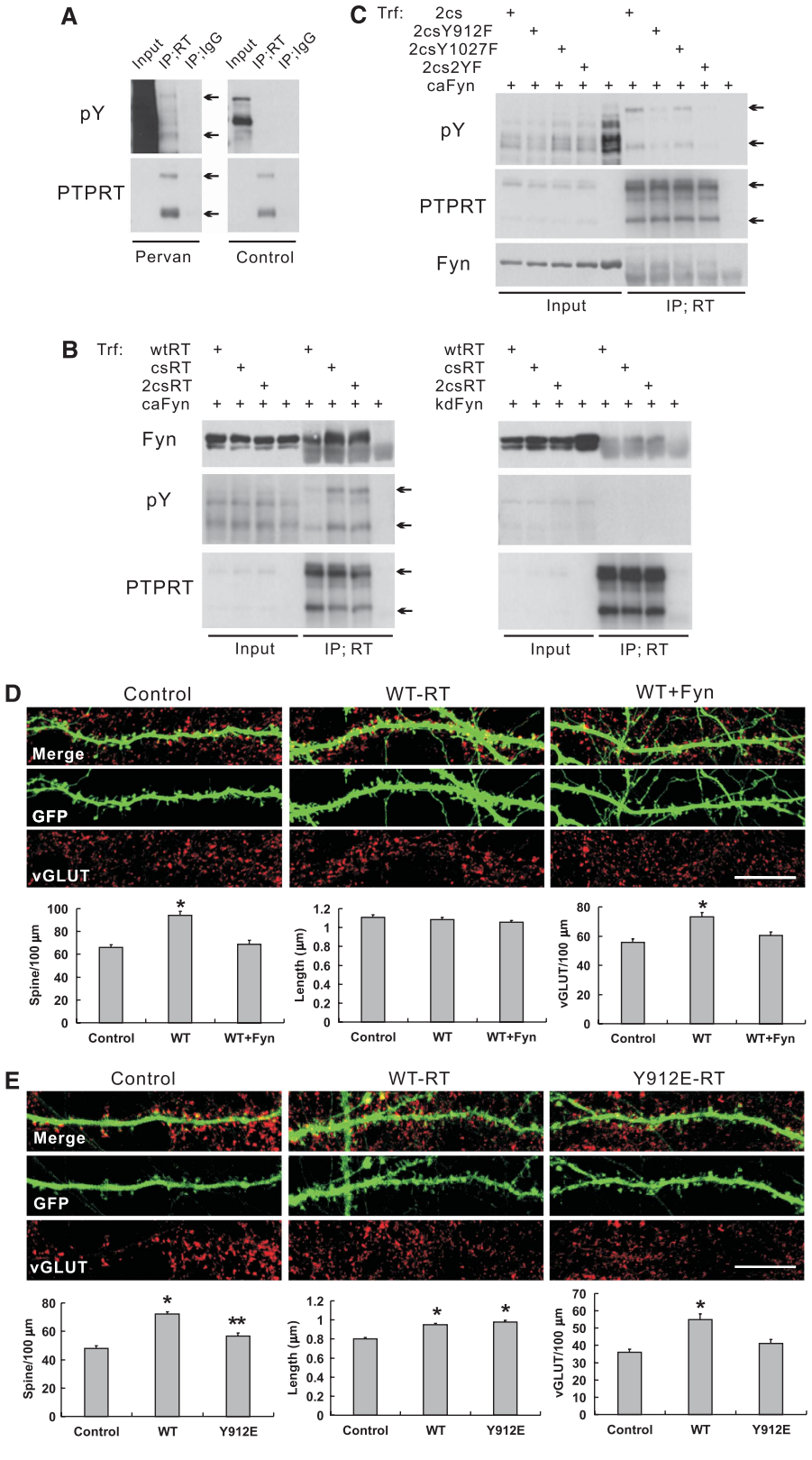

between amino acid residues 26 and 27 of PTPRT. For the construction of Fc-fusion proteins, the ecto-domain of PTPRT was fused with human Fc domain at the C-terminus. For siRNA knockdown, nt 3188–3206 and nt 2685–2703 of rat PTPRT (CGGAACCATGACAAGAACC, RTsiRNA#1; GAAAGGCTACCATGAG ATC, RTsiRNA#2; NM_001108603) were subcloned into pSuper.gfp/neo (OligoEngine). The C1103S (cs), C1103,1397S (2cs), Y912E, Y1027E, Y912,1027E, Y912F, Y1027F, Y912,1027F, and K635N, R637L PTPRT constructs were generated by site-directed mutagenesis using the Quick-Change system (Stratagene). The mouse RPTPκ construct was kindly provided by Dr Sap (Universite Paris Diderot Paris 7, France). The human PTPRM and PTPRU (PCP-2) constructs were generously donated by Dr Brady-Kalnay and Dr Wang (Case Western Reserve University, USA). The Fyn constructs (Fyn Y531F, constitutively active and Fyn K299M, kinase dead) were generously provided by Dr Yamamoto (University of Tokyo, Japan). The YFP-neuroligins and CFP-neurexins were kindly donated by Dr Craig (University of British Columbia, Canada).

Antibodies

The PTPRT monoclonal antibody was raised against the catalytic domain (aa 908–1164) as an antigen. A PTPRT-specific clone was selected by ELISA using purified antigen, and the ascites was produced in mice. The PTPRT polyclonal antibody was produced against the juxta-membrane domain (aa 804–966) as an antigen in the guinea-pig. Two peptide epitopes of neurexin 2α (RGRSPTMRDSTTQN and KAPAAPKTPSKAKK) were used for the production of a polyclonal antibody in rabbit. The SK-7 antibody was generously provided by Dr Brady-Kalnay (Case Western Reserve University, USA). Other antibodies were purchased from commercial sources: synapsin1, vGLUT, vGAT, neuroligin1, neuroligin2, and neurexin (Synaptic Systems GmbH); 4G10 (anti-phosphotyrosine, Upstate); Fyn and β-catenin (Santa Cruz); MAP2 and FLAG (Sigma); GFAP (Abcam).

Cell culture and transfection

HEK293T cells, maintained in DMEM containing 10% foetal bovine serum, were transfected by the calcium phosphate method. Primary hippocampal neuronal cultures were as described earlier and transfected by the calcium phosphate method (Lee *et al*, 2004).

Subcellular fractionation

Rat brain homogenates (H in Figure 1C) were centrifuged at 900 *g* to remove nuclei and other large debris (P1). The supernatant was centrifuged at 12 000 *g* to obtain a crude synaptosomal fraction (P2). The supernatant (S2) was centrifuged at 250 000 *g* to obtain light membrane (P3) and cytosolic fraction (S3). In parallel, the P2 fraction was subjected to hypotonic lysis and centrifuged at 25 000 *g* to precipitate synaptosomal membrane (LP1). The supernatant (LS1) was further centrifuged at 250 000 *g* to obtain a crude synaptic vesicle-enriched fraction (LP2) and soluble fraction (LS2). To obtain PSD fractions, the synaptosomal fraction was extracted with detergents, once with Triton X-100 (PSD I), twice with Triton X-100 (PSD II), once with Triton X-100, and once with sarcosyl (PSD III).

Immunoprecipitation and mass spectrometry

PTPRT-specific monoclonal antibody was used for immunoprecipitation in rat brain synaptosomal fraction. A total of 8 mg sodium deoxychorate-extracted synaptosome (P2-DOC) was incubated with 80 μl mouse ascites for immunoprecipitation. The resulting complex was pulled down by protein G-agarose beads, and proteins were separated from the resin by boiling with SDS-sampling buffer. Samples were resolved with 10% SDS–PAGE and stained by Coomassie blue staining. Approximately 50 SDS-gel bands were excised, destained, and digested with trypsin. The resultant peptide mixtures were analysed by online liquid chromatography/tandem mass spectrometry (Waters nanoACQUITY/Q-Tof Premier, Milford, USA) to generate peptide sequence information. Two intense ions, which met the predetermined MS survey scan criteria, were selected for collision-induced fragmentation. The collision energy of the selected ion was automatically determined according to its charge and mass. The acquisition software collected MS/MS spectra for 7 s for each selected ion, and then acquisition was returned to MS survey mode. The mass spectral data were processed into peak lists containing m/z values, charge states of the parent ion, fragment ion masses, and intensities, and these were then correlated with protein sequence databases using Mascot software (Matrix Science, London, UK). Proteins were identified on the basis of matching the MS/MS data with mass values calculated for selected ion series of a peptide.

Competition with soluble PTPRT ecto-Fc

The ecto-domains of PTPRT (aa 1–749 or 1–763) were fused to the Fc region of human immunoglobulin (RT-ecto-Fc) and Fc-fusion proteins were purified in HEK293T cell maintained in serum-free culture medium. Cultured neurons transfected with pSuper.gfp/neo (for visualization of dendritic protrusions; days in vitro (DIV) 9–20) were treated with RT-ecto-Fc for 4 days (4 μg/ml).

Image acquisition and quantification

Images captured by confocal microscopy (LSM Meta, Zeiss) were analysed blindly using MetaMorph software (Universal Imaging). The density of dendritic protrusions (0.4–2.5 μm) and synaptic protein clusters was measured from 40–50 dendrites of 8–10 neurons; the total dendritic length of ~50 μm was measured from the first dendritic branching points. Means from multiple individual dendrites were averaged to obtain a population mean and s.e.m.

In vitro tyrosine phosphatase assay

Recombinant proteins containing the PTPRT catalytic domain (aa 886–1164 into pET28a) were produced and purified by affinity and size-exclusion chromatography. PTP activity was assayed with 6,8-difluoro-4-methylumbelliferyl phosphate (DiFMUP, Molecular Probe) as a substrate. The reaction was performed for 20 min at room temperature and stopped by adding 1 mM sodium orthovanadate. Fluorescence excitation of hydrolysed DiFMUP was measured at 355 nm, and emission was detected at 460 nm in a fluorescence plate reader.

Supplementary data

Supplementary data are available at *The EMBO Journal* Online (http://www.embojournal.org).

Figure 6 Attenuation of synapse formation by PTPRT tyrosine phosphorylation. (**A**) Tyrosine phosphorylation of PTPRT in cultured neurons. DIV21 rat hippocampal neurons were solubilized and endogenous PTPRT was immunoprecipitated. When cultured neurons were treated with pervanadate, the tyrosine residue of PTPRT was phosphorylated (arrow). Input, 5%. (**B**) Co-immunoprecipitation with Fyn and PTPRT. In heterologous cells, PTPRT and Fyn were transfected to evaluate if they interact. Using PTPRT antibodies, constitutively active Fyn (caFyn) was recruited, but the kinase-dead Fyn (kdFyn) was not. Note that the phospho-tyrosine level of wild-type PTPRT (WT-RT) was reduced compared with the activity-dead PTPRT (csRT & 2csRT) (arrow). Input, 1.5%. (**C**) Major tyrosine residues of PTPRT phosphorylated by Fyn. As the 912 and 1027 tyrosine residues of PTPRT were candidates for phosphorylation, they were mutated to phenylalanine and co-transfected with Fyn. The phospho-tyrosine level of Y912F-RT was substantially decreased in contrast to those of WT and Y1027F-RT (arrow). For comparison, YF mutants were constructed in inactive 2cs-RT. Input, 1.5%. (**D**) Decreased synapse formation by co-expression with Fyn. PTPRT-induced synapse formation was attenuated by co-expression of Fyn. The density of dendritic spines and excitatory synapses decreased when PTPRT was co-transfected with Fyn compared with WT PTPRT single transfection. Mean ± s.e.m. $n = 52$ dendrites for control, 43 for WT-RT, and 41 for WT-RT + Fyn. $^*P < 0.0001$ (Student's *t*-test). Scale bar, 10 μm. (**E**) Inhibition of synapse formation by phospho-mimic mutants. Tyrosine residue 912 was mutated to glutamate to mimic phosphorylation and expressed in cultured neurons. Synapse formation by Y912E-PTPRT was attenuated compared to WT PTPRT. Mean ± s.e.m. $n = 41$ dendrites for control, 30 for WT-RT, and 30 for Y912E-RT. $^*P < 0.0001$ and $^{**}P < 0.05$ (Student's *t*-test). Scale bar, 10 μm.

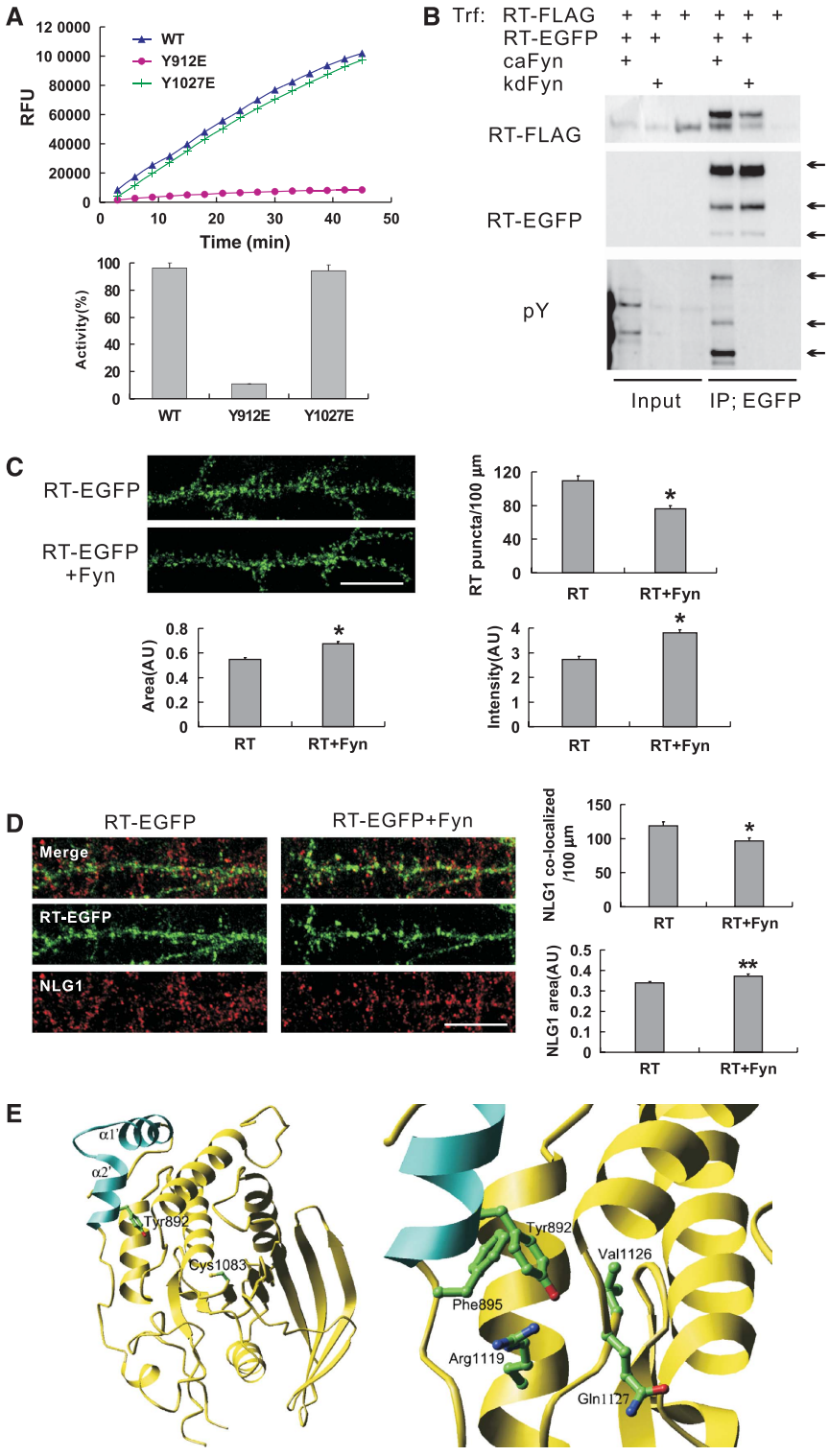

Figure 7 Decreased PTP activity and attenuated PTPRT–neuroligin interaction by PTPRT tyrosine phosphorylation. (**A**) PTP activity was reduced by the Y912E mutation. An *in vitro* PTP assay was performed using DiFMUP as substrate. The Y912E catalytic domain mutant showed significantly reduced PTP activity compared with wild type and Y1027 mutants. The slope was described as activity. (**B**) Increased homophilic interaction of PTPRT as a result of phosphorylation by Fyn. Two different tagged PTPRTs (EGFP and FLAG) interact strongly when phosphorylated by Fyn (arrow). Input, 1.5%. (**C**) PTPRT-EGFP clustering was enhanced by Fyn. The number of PTPRT puncta was decreased when Fyn was co-expressed in cultured neurons. The area and intensity of PTPRT puncta were increased by Fyn. Mean ± s.e.m. $n = 46$ frames for PTPRT single transfection, 48 for PTPRT and Fyn co-transfection. $^{*}P < 0.0001$ (Student's *t*-test). Scale bar, 10 μm. (**D**) Co-localization of PTPRT and neuroligin was decreased by Fyn. The number of neuroligin within PTPRT-EGFP puncta was decreased and neuroligin puncta were enlarged somewhat by Fyn co-expression. Mean ± s.e.m. $n = 30$ dendrites for PTPRT single transfection, 28 for PTPRT and Fyn co-transfection. $^{*}P < 0.005$ and $^{**}P < 0.01$ (Student's *t*-test). Scale bar, 10 μm. (**E**) Left, Overall view of PTPRK (RPTPκ) D1 catalytic domain. The wedge moiety is shown as cyan, whereas the rest of the molecule shown as yellow. The catalytic cysteine and the tyrosine residue are coloured green. Right, Close-up view of PTPRK near Y892. The residues involving the close contacts with Y892 are shown as sticks.

Acknowledgements

We thank Dr Ann Marie Craig for the kind gifts of neuroligin and neurexin expression constructs, Dr Tadashi Yamamoto for providing Fyn expression constructs, Dr Jan Sap for generous gifts of RPTPκ plasmids, and Dr Brady-Kalnay for kind donation of RPTPmu, PCP-2 plasmids, and antibodies. This work was supported by the Korea Science and Engineering Foundation (KOSEF), a grant funded by the Korea government (MOST) (R01-2007-000-11499-0 to J-RL), the KRIBB research initiative programme to J-RL, and the joint research collaboration programme for Chinese–Korean–Japanese research cooperation to D-YY.

Conflict of interest

The authors declare that they have no conflict of interest.

References

Alonso A, Sasin J, Bottini N, Friedberg I, Osterman A, Godzik A, Hunter T, Dixon J, Mustelin T (2004) Protein tyrosine phosphatases in the human genome. *Cell* **117:** 699–711

Anders L, Mertins P, Lammich S, Murgia M, Hartmann D, Saftig P, Haass C, Ullrich A (2006) Furin-, ADAM 10-, and γ-secretase-mediated cleavage of a receptor tyrosine phosphatase and regulation of β-catenin's transcriptional activity. *Mol Cell Biol* **26:** 3917–3934

Arac D, Boucard AA, Ozkan E, Strop P, Newell E, Sudhof TC, Byunger AT (2007) Structures of neuroligin-1 and the neuroligin-1/neurexin-1β complex reveal specific protein-protein and protein-Ca^{2+} interactions. *Neuron* **56:** 992–1003

Aricescu AR, Siebold C, Choudhuri K, Chang VT, Lu W, Davis SJ, Anton van Merwe P, Jones EY (2007) Structure of a tyrosine phosphatase adhesive interaction reveals a spacer-clamp mechanism. *Science* **317:** 1217–1220

Barford ZJ, Flint AJ, Tonks NK (1995) Structural basis for phosphotyrosine peptide recognition by protein tyrosine phosphatase 1B. *Science* **268:** 1754–1758

Berman-Golan D, Elson A (2007) Neu-meditated phosphorylation of protein tyrosine phosphatase epsilon is critical for activation of Src in mammary tumor cells. *Oncogene* **26:** 7028–7037

Besco J, Huijsduijnen R, Frostholm A, Rotter A (2006) Intracellular substrates of brain-enriched receptor protein tyrosine phosphatase rho (RPTPρ/PTPRT). *Brain Res* **1116:** 50–57

Besco J, Popesco MC, Davuluri RV, Frostthlm A, Rotter A (2004) Genomic structure and alternative splicing of murine R2B receptor protein tyrosine phosphatases (PTPκ, μ, ρ and PCP-2). *BMC Genomics* **5:** 14–32

Bilwes AM, den Hertog J, Hunter T, Noel JP (1996) Structural basis for inhibition of receptor protein-tyrosine phosphatase-α by dimerization. *Nature* **382:** 555–559

Blanchetot C, Tertoolen LGJ, den Hertog J (2002) Regulation of receptor protein-tyrosine phosphatase α by oxidative stress. *EMBO J* **21:** 493–503

Bodrikov V, Leshchyns'ka I, Sytnyk V, Overvoorde J, den Hertog J, Schachner M (2005) RPTPα is essential for NCAM-mediated $p59^{fyn}$ activation and neurite elongation. *J Cell Biol* **168:** 127–139

Boggon TJ, Murray J, Chappuis-Flament S, Wong E, Gumbiner BM, Shapiro L (2002) C-cadherin ectodomain structure and implications for cell adhesion mechanism. *Science* **296:** 1308–1313

Boucard AA, Chubykin AA, Comoletti D, Taylor P, Sudhof TC (2005) A splice code for *trans*-synaptic cell adhesion mediated by binding of neuroligin 1 to α- and β-neurexins. *Neuron* **48:** 229–236

Brady-Kalnay SM, Rimm DL, Tonks NK (1995) Receptor protein tyrosine phosphatase PTPμ associates with cadherins *in vivo*. *J Cell Biol* **130:** 977–986

Burden-Gulley SM, Brady-Kalnay SM (1999) PTPμ regulates N-cadherin-dependent neurite outgrowth. *J Cell Biol* **144:** 1323–1336

Chih B, Engelman H, Scheiffele P (2005) Control of excitatory and inhibitory synapse formation by neuroligins. *Science* **307:** 1324–1328

Chubykin AA, Atasoy D, Etherton MR, Brose N, Kavalali ET, Gibson JR, Sudhof TC (2007) Activity-dependent validation of excitatory versus inhibitory synapses by neuroligin-1 versus neuroligin-2. *Neuron* **54:** 919–931

Comoletti D, Grishaev A, Whitten AE, Tsigelny I, Taylor P, Trewhella J (2007) Synaptic arrangement of the neuroligin/β-neurexin complex revealed by X-ray and neutron scattering. *Structure* **15:** 693–705

Craig AM, Kang Y (2007) Neurexin-neuroligin signaling in synapse development. *Curr Opin Neurol* **17:** 43–52

Dean C, Dresbach T (2006) Neuroligins and neurexins: linking cell adhesion, synapse formation and cognitive function. *Trends Neurosci* **29:** 21–29

Dean C, Sholl FG, Choih J, DeMaria S, Berger J, Isacoff E, Scheiffele P (2003) Neurexin mediates the assembly of presynaptic terminals. *Nat Neurosci* **6:** 708–716

Dunah AW, Hueske E, Wyszynski M, Hoogenraad CC, Jaworski J, Pak DT, Simonetta A, Liu G, Sheng M (2005) LAR receptor protein tyrosine phosphatases in the development and maintenance of excitatory synapses. *Nat Neurosci* **8:** 458–467

Eswaran J, Debreczeni JE, Longman E, Barr AJ, Knapp S (2006) The crystal structure of human receptor protein tyrosine phosphatase κ phosphatase domain 1. *Protein Sci* **15:** 1500–1505

Gebbink MFBG, Zondag GCM, Koningstein GM, Feiken E, Wubbolts RW, Moolenaar WH (1995) Cell surface expression of receptor protein tyrosine phosphatase RPTPμ is regulated by cell-cell contact. *J Cell Biol* **131:** 251–260

Graf ER, Zhang X, Jin SX, Linoff MW, Craig AM (2004) Neurexins induce differentiation of GABA and glutamate postsynaptic specializations via neuroligins. *Cell* **119:** 1013–1026

Harroch S, Palmeri M, Rosenbluth J, Custer A, Okigaki M, Shrager P, Blum M, Buxbaum JD, Schlessinger J (2000) No obvious abnormality in mice deficient in receptor protein tyrosine phosphatse β. *Mol Cell Biol* **20:** 7706–7715

Hoffmann K, Tonks NK, Barford D (1997) The crystal structure of domain 1 of receptor protein-tyrosine phsophatase μ. *J Biol Chem* **272:** 27505–27508

Husi H, Ward MA, Choudhary JS, Blackstock WP, Grant SGN (2000) Proteomic analysis of NMDA receptor-adhesion protein signaling complexes. *Nat Neurosci* **3:** 661–669

Jamain S, Quach H, Betancur C, Rastam M, Colineaux C, Gillberg IC, Soderstrom H, Giros B, Leboyer M, Gillberg C (2003) Mutations of the X-linked genes encoding neuroligins NLG3 and NLG4 are associated with autism. *Nat Genet* **34:** 27–29

Jiang YP, Wang H, D'Eustachio P, Musacchio JM, Schlessinger J, Sap J (1993) Cloning and characterization of R-PTP-κ, a new member of the receptor protein tyrosine phosphatase family with a proteolytically cleaved cellular adhesion molecule-like extracellular region. *Mol Cell Biol* **13:** 2942–2951

Johnson KG, Van Vactor D (2003) Receptor protein tyrosine phosphatases in nervous system development. *Physiol Rev* **83:** 1–24

Kim S, Burette A, Chung HS, Kwon SK, Woo J, Lee HW, Kim K, Kim H, Weinberg RJ, Kim E (2006) NGL family PSD-95-interacting adhesion molecules regulate excitatory synapse formation. *Nat Neurosci* **9:** 1294–1301

Krasnoperov V, Bittner M, Mo W, Buryanovsky L, Neubert T, Holz RW, Ichtchenko K, Petrenko AG (2002) Protein-tyrosine phosphatase-σ is a novel member of the functional family of α-latrotoxin receptors. *J Biol Chem* **277:** 35887–35895

Lee JR, Shin H, Choi J, Ko J, Kim S, Lee HW, Kim K, Rho SH, Lee JH, Song HE, Eom SH, Kim E (2004) An intramolecular interaction between the FHA domain and a coiled coil negatively regulates the kinesin motor KIF1A. *EMBO J* **23:** 1506–1515

Liu H, Nakazawa T, Tezuka T, Yamamoto T (2006) Physical and functional interaction of Fyn tyrosine kinase with a brain-enriched Rho GTPase-activating protein TCGAP. *J Biol Chem* **281:** 23611–23619

McAndrew PE, Frostholm A, Evans JE, Zdilar D, Goldowitz D, Chiu IM, Burghes AHM, Rotter A (1998) Novel receptor protein tyrosine phosphatase (RPTPρ) and acidic fibroblast growth factor (FGF-1) transcripts delineate a rostrocaudal boundary in the granule cell layer of the murine cerebellar cortex. *J Comp Neurol* **391:** 444–455

Mustelin T, Altman A (1990) Dephosphorylation and activation of the T cell tyrosine kinase pp56lck by the leukocyte common antigen(CD45). *Oncogene* **5:** 809–813

Nam HJ, Poy F, Krueger NX, Saito H, Frederick CA (1999) Crystal structure of the tandem phosphatase domains of RPTP LAR. *Cell* **97:** 449–457

Nam HJ, Poy F, Krueger NX, Saito H, Frederick CA (2005) Structural basis for the function and regulation of the receptor protein tyrosine phosphatase CD45. *J Exp Med* **201:** 441–452

Paul S, Lombroso PJ (2003) Receptor and nonreceptor protein tyrosine phosphatases in the nervous system. *Cell Mol Life Sci* **60:** 2465–2482

Petrone A, Battaglia F, Wang C, Dusa A, Su J, Zagzag D, Bianchi R, Casaccia-Bonnefil P, Arancio O, Sap J (2003) Receptor protein tyrosine phosphatase α is essential for hippocampal neuronal migraton and long-term potentiation. *EMBO J* **22:** 4121–4131

Sallee JL, Wittchen ES, Burridge K (2006) Regulation of cell adhesion by protein-tyrosine phosphatases. II. Cell-cell adhesion. *J Biol Chem* **281:** 16189–16192

Shintani T, Ihara M, Sakuta H, Takahashi H, Watakabe I, Noda M (2006) Eph receptors are negatively controlled by protein tyrosine phosphatase receptor type O. *Nat Neurosci* **9:** 761–769

Sudhof TC (2008) Neuroligins and neurexins link synaptic function to cognitive disease. *Nature* **455:** 903–911

Tsujikawa K, Ichijo T, Moriyama K, Tadotsu N, Sakamoto K, Sakane N, Fukada S, Furukawa T, Saito H, Yamamoto H (2002) Regulation of Lck and Fyn tyrosine kinase activities by transmembrane protein tyrosine phosphatase leukocyte common antigen-related molecule. *Mol Cancer Res* **1:** 155–163

Uetani N, Chagnon MJ, Kennedy TE, Iwakura Y, Tremblay ML (2006) Mammalian motoneuron axon targeting requires receptor protein tyrosine phosphatase σ and δ. *J Neurosci* **2006:** 5872–5880

van Montfort RLM, Congreve M, Tisi D, Carr R, Jhoti H (2003) Oxidation state of the active-site cysteine in protein tyrosine phosphatase 1B. *Nature* **423:** 773–777

Vogel W, Lammers R, Huang J, Ullrich A (1993) Activation of a phosphotyrosine phosphatase by tyrosine phosphorylation. *Science* **259:** 1611–1614

Wang Z, Shen D, Parsons DW, Bardelli A, Sager J, Szabo S, Ptak J, Silliman N, Peters BA, van der Heijden MS, Parmigiani G, Yan H, Wang TL, Riggins G, Powell SM, Wilson KV, Markowitz S, Kinzler KW, Vogelstein B, Velculescu VE (2004) Mutational analysis of the tyrosine phosphatome in colorectal cancers. *Science* **304:** 1164–1166

Woo J, Kwon SK, Choi S, Kim S, Lee JR, Dunah A, Sheng M, Kim E (2009) Trans-synaptic adhesion between NGL-3 and LAR regulates the formation of excitatory synapses. *Nat Neurosci* **12:** 428–437

Xie Y, Yeo TT, Zhang C, Yang T, Tisi MA, Massa SM, Longo FM (2001) The leukocyte common antigne-related tyrosine phosphatase receptor regulates regenerative outgrowth *in vivo*. *J Neurosci* **21:** 5130–5138

Zeng L, D'Alessamdri L, Kalousek MB, Vaughan L, Pallen CJ (1999) Protein tyrosine phosphatase α (PTPα) and contactin form a novel neuronal receptor complex linked to the intracellular tyrosine kinase Fyn. *J Cell Biol* **147:** 707–713

Zhang X, Guo A, Yu J, Possemato A, Chen Y, Zheng W, Polakiewicz RD, Kinzler KW, Vogelstein B, Velculescu VE, Wang ZJ (2007) Identification of STAT3 as a substrate of receptor protein tyrosine phosphatase T. *Proc Natl Acad Sci* **104:** 4060–4064

Zheng XM, Resnick RJ, Shalloway D (2000) A phosphotyrosine displacement mechanism for activation of Src by PTPα. *EMBO J* **19:** 964–978

Zondag GCM, Koningstein GM, Jiang YP, Sap J, Moolenaar WH, Gebbink MFBG (1995) Homophilic interactions mediated by receptor tyrosine phosphatase μ and κ. *J Biol Chem* **270:** 14247–14250

